Chirp-free optical return-to-zero modulation based on a single microring resonator

Lili Sun, Tong Ye,* Xiaowen Wang, Linjie Zhou, and Jianping Chen

Department of Electronic Engineering, State Key Laboratory of Advanced Optical Communication Systems and Networks, Shanghai Jiao Tong University, Shanghai, 200240, China

*yetong@sjtu.edu.cn

Abstract: This paper proposes a chirp-free optical return-to-zero (RZ) modulator using a double coupled microring resonator. Optical RZ modulation is achieved by applying a clock (CLK) driving signal to the input coupling region and a non-return-to-zero (NRZ) driving signal to the output coupling region. Static and time-domain coupled-mode theory (CMT) based dynamic analyse are performed to theoretically investigate its performance in RZ modulation. The criteria to realize RZ modulation are deduced. Various RZ modulation formats, including RZ phase-shift-keying (RZ-PSK), carrier-suppressed RZ (CSRZ), and RZ intensity modulation formats, can be implemented by using CLK and NRZ signals with different combinations of polarities. Numerical simulations are performed and the feasibility of our modulator at 10 Gbit/s for the multiple RZ modulation formats is verified.

OCIS codes: (060.0060) Fiber optics and optical communications; (060.4080) Modulation; (130.0130) Integrated optics.

References and links

1. P. J. Winzer and R. J. Essiambre, "Advanced optical modulation formats," Proc. IEEE **94,** 952–985 (2006).
2. Q. Xu, B. Schmidt, S. Pradhan, and M. Lipson, "Micrometre-scale silicon electro-optic modulator," Nature **435,** 325–327 (2005).
3. S. Manipatruni, X. Qianfan, B. Schmidt, J. Shakya, and M. Lipson, "High speed carrier injection 18 Gb/s silicon micro-ring electro-optic modulator," in *Proceedings of Lasers and Electro-Optics Society* (IEEE, 2007), 537–538.
4. W. D. Sacher, W. M. Green, S. Assefa, T. Barwicz, S. M. Shank, Y. A. Vlasov, and J. Poon, "Controlled coupling in silicon microrings for high-speed, high extinction ratio, and low-chirp modulation," in *CLEO:2011 - Laser Applications to Photonic Applications to Photonic Applications*, OSA Technical Digest (CD) (Optical Society of America, 2011), paper PDPA8.
5. K. Padmaraju, N. Ophir, S. Manipatruni, C. B. Poitras, M. Lipson, and K. Bergman, "DPSK modulation using a microring modulator," in *CLEO:2011 - Laser Applications to Photonic Applications*, OSA Technical Digest (CD) (Optical Society of America, 2011), paper CTuN4.
6. L. Zhang, Y. Li, J. Yang, R. G. Beausoleil, and A. E. Willner, "Creating RZ data modulation formats using parallel silicon microring modulators for pulse carving in DPSK," in *Conference on Lasers and Electro-Optics/Quantum Electronics and Laser Science Conference and Photonic Applications Systems Technologies*, OSA Technical Digest (CD) (Optical Society of America, 2008), paper CWN4.
7. A. Yariv, "Critical coupling and its control in optical waveguide-ring resonator systems," IEEE Photon. Technol. Lett.**14,** 483–485 (2002).
8. B. E. Little, S. T. Chu, H. A. Haus, J. Foresi, and J.-P. Laine, "Microring resonator channel dropping filters," J. Lightwave Technol.**15,** 998–1005 (1997).

#160060 - $15.00 USD Received 15 Dec 2011; revised 31 Jan 2012; accepted 16 Feb 2012; published 20 Mar 2012

9. L. Zhang, Y. Li, J.-Y. Yang, M. Song, R. G. Beausoleil, and A. E. Willner, "Silicon-based microring resonator modulators for intensity modulation," IEEE J. Sel. Top. Quantum Electron.**16,** 149–158 (2010).
10. H. A. Haus, *Waves and fields in optoelectronics* (Prentice-Hall Englewood Cliffs, 1985).
11. H. Park, M. N. Sysak, H.-W. Chen, A. W. Fang, D. Liang, L. Liao, B. R. Koch, J. Bovington, Y. Tang, K. Wong, M. Jacob-Mitos, R. Jones, and J. E. Bowers, "Device and Integration Technology for Silicon Photonic Transmitters," IEEE Sel. Top. Quantum Electron.**17,** 671–688 (2011).
12. M. Hochberg, T. Baehr-Jones, G. Wang, J. Huang, P. Sullivan, L. Dalton, and A. Scherer, "Towards a millivolt optical modulator with nano-slot waveguides," Opt. Express **15,** 8401–8410 (2007).
13. C. Angulo Barrios, V. R. Almeida, R. Panepucci, and M. Lipson, "Electrooptic modulation of silicon-on-insulator submicrometer-size waveguide devices," J. Lightwave Technol. **21,** 2332- (2003).
14. L. Ghisa, Y. Dumeige, N. N. T. Kim, Y. G. Boucher, and P. Feron, "Performances of a fully integrated all-optical pulse reshaper based on cascaded coupled nonlinear microring resonators," J. Lightwave Technol. **25,** 2417–2426 (2007).

1. Introduction

Non-return-to-zero (NRZ) and return-to-zero (RZ) are important modulation formats in optical transmission systems. The NRZ modulation format, widely used in short-reach networks, requires less bandwidth and has higher timing tolerance. The RZ modulation format, though requiring a more complex modulation scheme, is more robust to intersymbol interferences (ISI) and nonlinear propagation distortions [1], and thus has better receiver sensitivity. Therefore, optical RZ modulators receive sustained attention from the optical communication society.

In recent years, microring-based modulators have been recognized as promising electro-optic modulators due to their potential for high-density integration. By controlling the refractive index of the ring waveguide [2, 3] or the coupling strength between the ring waveguide and the bus waveguide [4], a single ring resonator can be employed to generate NRZ signals and NRZ phase-shift-keying (PSK) signals. For example, a silicon microring with a diameter of 12 μm was reported in Ref. [3] to perform the NRZ intensity modulation at 18 Gb/s, and the NRZ-PSK modulation at 250-Mb/s was demonstrated in Ref. [5]. However, previous work mainly focuses on the generation of NRZ-type modulation formats, and little attention is paid to realizing the RZ modulation based on microring resonators. Up to now, to our knowledge, there is only one scheme [6] that was proposed to generate low-chirp RZ-PSK signals using three microring resonators.

In this paper, we propose a method to perform chirp-free RZ modulations using a single microring resonator side-coupled to two straight waveguides. To implement the RZ modulation, the coupling coefficients of the couplers at the input and output sides are independently controlled by an electrical clock (CLK) signal and an NRZ signal. In this case, if continuous wave (CW) light at the resonance wavelength is injected to the input waveguide, one can obtain an optical RZ signal at the output waveguide. Moreover, our dynamic analysis and simulation demonstrate that the proposed microring-based modulator is able to generate multiple RZ modulation formats, including RZ, carrier-suppressed RZ (CSRZ), and RZ-PSK, if the polarities of the driving signals are properly adjusted.

2. Principle

2.1. Static analysis

The schematic structure of the proposed modulator is given in Fig. 1(a). The modulator is composed by a microring resonator side-coupled to a pair of straight waveguides. The CW light from the input port successively passes through the input and output coupling regions before being detected at the drop port. The optical field transfer matrix at the input and output

#160060 - $15.00 USD Received 15 Dec 2011; revised 31 Jan 2012; accepted 16 Feb 2012; published 20 Mar 2012

coupling regions is given as

$$M_i = e^{-j\theta_i} \begin{pmatrix} t_i & -jk_i \\ -jk_i & t_i \end{pmatrix}, \tag{1}$$

where the subscript $i = 1,\ 2$ represents the input and output couplers, θ_i is the propagation phase-shift for the coupler, t_i is the self-coupling coefficient, and k_i is the cross-coupling coefficient. In the lossless case, $t_i^2 + k_i^2 = 1$.

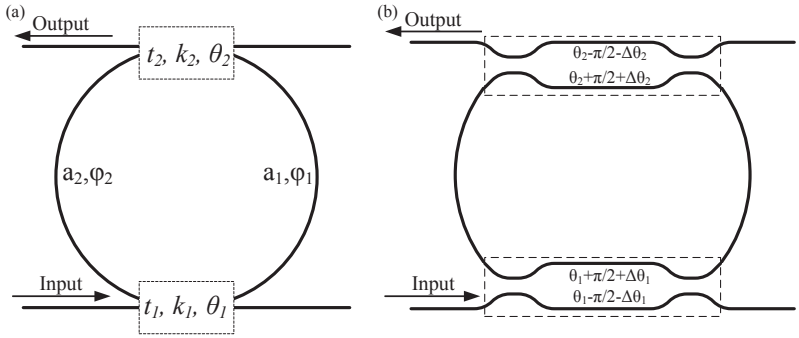

Fig. 1. Schematics of a coupling modulated microring resonator for (a) the general case and (b) two MZI couplers.

Let a_1 and a_2 be the propagation losses of ring waveguides, φ_1 and φ_2 be the phase-shifts of the ring waveguides. The microring resonator transfer function can be expressed as follows:

$$T_{drop} = \frac{-k_1 k_2 a_1 e^{-j(\theta_1+\theta_2+\varphi_1)}}{1 - t_1 t_2 a_1 a_2 e^{-j(\theta_1+\theta_2+\varphi_1+\varphi_2)}}. \tag{2}$$

At resonance wavelengths, $e^{-j(\theta_1+\theta_2+\varphi_1+\varphi_2)} = 1$, and Eq. (2) becomes

$$T_{drop} = \frac{-k_1 k_2 a_1 e^{j\varphi_2}}{1 - t_1 t_2 a_1 a_2}. \tag{3}$$

If $k_1,\ k_2 \ll 1$, Eq. (3) can reduce to

$$T_{drop} \approx \frac{-a_1 e^{j\varphi_2}}{1 - a_1 a_2} k_1 k_2. \tag{4}$$

It clearly indicates that one can obtain an optical RZ signal, if the two coupling coefficients are respectively modulated by an electrical NRZ and a CLK signal with the assumption $k_1,\ k_2 \ll 1$. We will show by simulations in Section 3 that the analytical results are still valid even when the small signal assumptions are relaxed.

To realize the coupling modulation, MZI couplers operated in a push-pull mode [7] can be used for these two coupling regions, as illustrated in Fig. 1(b). The coupling coefficients can then be expressed as $k_i = je^{-j\theta_i} \sin\Delta\theta_i$, where θ_i is the phase-shift induced by the MZI coupler.

2.2. Dynamic analysis

The static analysis has suggested the possibility of RZ modulations using a single ring, whereas the result is only valid for the low-frequency modulations. To explore the performance at high modulation frequency, we analyze its dynamic performance using the time-domain coupled-mode theory (CMT) [8]. In the CMT analysis, the microring resonator is regarded as a lumped

#160060 - $15.00 USD Received 15 Dec 2011; revised 31 Jan 2012; accepted 16 Feb 2012; published 20 Mar 2012

element with a time-varying optical energy amplitude a. When light is launched on resonance, the resonator optical energy change rate is given as:

$$\frac{da(t)}{dt} = (j\omega_0 - \frac{1}{\tau_l} - \frac{1}{\tau_e} - \frac{1}{\tau_d})a(t) - j\sqrt{\frac{v_g}{L}}k_1 e^{j\omega_0 t} \tag{5}$$

where L is the perimeter of the ring resonator, ω_0 is the resonant frequency, $1/\tau_l$ is the resonator intrinsic decay rate, $1/\tau_e = v_g k_1^2/2L$ and $1/\tau_d = v_g k_2^2/2L$ are the decay rates due to the input and output couplings, and v_g is the light group velocity in the waveguide. The signal wave amplitude transmitted to the drop port s_d is related to a as follows [9]:

$$s_d = -j\sqrt{\frac{v_g}{L}}k_2 a. \tag{6}$$

Suppose two electrical driving signals are applied to the input and output coupling regions, the refractive indices are modulated as $n_i(t) = n \pm (m_{b_i} + m_i \cos\omega_i t)$, where m_{b_i} is the bias, m_i is the modulation amplitude, and ω_i is the angular frequency of the applied electrical signal. Thereby, the input and output cross-coupling coefficients are modulated as

$$k_i(t) = \sin[(m_{b_i} + m_i \cos\omega_i t)\beta L_e/n] \approx k_{b_i} + r_{b_i}\cos\omega_i t,\ i = 1,2 \tag{7}$$

where $k_{b_i} = \sin(m_{b_i}\beta L_e/n)$, $r_{b_i} = m_i(\beta L_e/n)\cos(m_{b_i}\beta L_e/n)$, $i = 1,2$, β is the propagation constant in the waveguide, and L_e is the MZI arm length.

Substituting $k_1(t)$ and $k_2(t)$ into Eq. (5) and solving Eqs. (5) and (6) with the small signal assumption $r_{b_1} \ll 1$ and $r_{b_2} \ll 1$, we have:

$$\begin{aligned} s_d(t) \quad \approx \quad & -\frac{v_g}{L}\left[\frac{k_{b_1}k_{b_2}}{\Omega} + \frac{k_{b_2}r_{b_1}}{\sqrt{\omega_1^2+\Omega^2}}\cos(\omega_1 t - \phi_1) + \frac{k_{b_1}r_{b_2}}{\Omega}\cos(\omega_2 t)\right] + \\ & \frac{{v_g}^2}{L^2}\frac{k_{b_1}k_{b_2}}{\Omega}\left[\sum_{i=1}^{2}\frac{k_{b_i}r_{b_i}}{\sqrt{\omega_i^2+\Omega^2}}\cos(\omega_i t - \phi_i)\right] \end{aligned} \tag{8}$$

where $\phi_i = \arcsin[\sqrt{\omega_i^2/(\omega_i^2+\Omega^2)}]$ and $\Omega = 1/\tau_l + (v_g/2L)(k_{b_1}^2 + k_{b_2}^2)$. It shows that the proposed modulation scheme is chirp-free since $s_d(t)$ is a real number. If $k_{b_1}k_{b_2} = 0$ (or $1/\tau_l \gg (v_g/2L)(k_{b_1}^2 + k_{b_2}^2)$) and $\omega_1 \ll \Omega$, Eq. (8) will immediately reduce to

$$s_d(t) \approx -\frac{v_g}{L}\frac{k_1(t-\phi_1/\omega_1)k_2(t)}{\Omega}. \tag{9}$$

Equation (9) indicates that it is feasible to use a single ring to realize RZ modulation, as long as the following criteria are satisfied:

1. ω_1 cannot be very high;
2. $k_{b_1}k_{b_2} = 0$ or $(1/\tau_l) \gg (v_g/2L)(k_{b_1}^2 + k_{b_2}^2)$, i.e., the unloaded quality factor (Q-factor) of the microring resonator cannot be very high;
3. Signal applied to the input coupling region needs to be shifted with a phase ϕ_1 in advance.

Condition 1 suggests that the modulation is inherently bandwidth-limited. Such characteristic is manifested by the Optical Modulation Amplitude (OMA), which is defined as:

$$OMA = \frac{f(t)_{max} - f(t)_{min}}{2}, \tag{10}$$

#160060 - $15.00 USD Received 15 Dec 2011; revised 31 Jan 2012; accepted 16 Feb 2012; published 20 Mar 2012

where $f(t)_{max}$ and $f(t)_{min}$ are the maximum and minimum amplitudes of the signal. In the case of our scheme,

$$OMA = \frac{v_g}{L}\left|k_{b_2}r_{b_1}\frac{\Omega - 2k_{b_1}^2\frac{v_g}{2L}}{\Omega\sqrt{\omega_1^2+\Omega^2}}\right| + \frac{v_g}{L}\left[(\frac{k_{b_1}r_{b_2}}{\Omega})^2 + \left(\frac{v_g}{2L}(2k_{b_1}k_{b_2}r_{b_2})^2\frac{k_{b_2}^2\frac{v_g}{2L}-\Omega}{\Omega^2(\omega_2^2+\Omega^2)}\right)\right]^{1/2}. \tag{11}$$

When $\omega_2 = 0$,

$$OMA|_{\omega_2=0} = \frac{v_g}{L}\left|k_{b_2}r_{b_1}\frac{\Omega - 2k_{b_1}^2\frac{v_g}{2L}}{\Omega\sqrt{\omega_1^2+\Omega^2}}\right|. \tag{12}$$

If $\omega_1 \to \infty$, $OMA|_{\omega_2=0}$ rapidly reduces to zero, as illustrated in Fig. 2(a). The roll-off frequency ω_{3dB} defined as the range of frequency where the OMA is reduced to $1/\sqrt{2}$ of the maximum frequency response. Clearly, we have $\omega_{3dB_1} = \Omega$ according to Eq. (12). Also, when $\omega_1 = 0$,

$$OMA|_{\omega_1=0} = \frac{v_g}{L}\left[(\frac{k_{b_1}r_{b_2}}{\Omega})^2 + \left(\frac{v_g}{2L}(2k_{b_1}k_{b_2}r_{b_2})^2\frac{k_{b_2}^2\frac{v_g}{2L}-\Omega}{\Omega^2(\omega_2^2+\Omega^2)}\right)\right]^{1/2}. \tag{13}$$

$OMA|_{\omega_1=0}$ almost keeps unchanged even when $\omega_2 \to \infty$, as shown in Fig. 2(b). This implies that: 1) The RZ modulation is bandwidth-limited at the input coupling region; 2) A square-wave NRZ signal, which has a broad frequency spectrum, may incur severe distortion if it is applied to the input coupling region. To minimize the signal distortion, we put the NRZ signal at the output coupling region and the CLK signal at the input coupling region, as illustrated in Fig. 3(a).

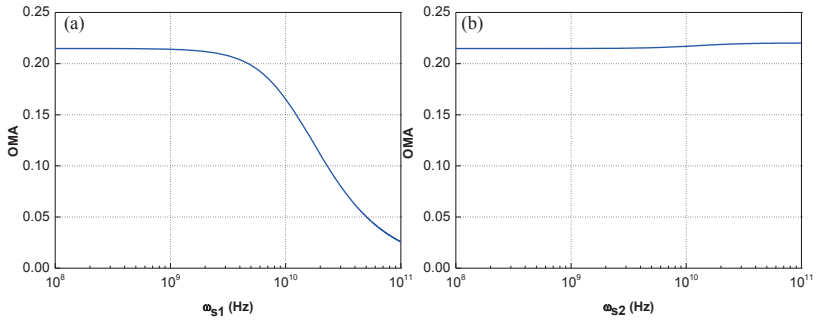

Fig. 2. OMA changes with signal frequency. (a) $m_{b_1} = m_1 = 10^{-4}$, $m_{b_2} = m_2 = 10^{-3}$ and $\omega_2 = 0$ (b) $m_{b_1} = m_1 = 10^{-3}$, $m_{b_2} = m_2 = 10^{-4}$ and $\omega_1 = 0$.

As for condition (2), we consider three cases. First, $k_{b_1} \neq 0$ and $k_{b_2} = 0$, i.e., the driving signal applied to the input coupling region is unipolar while the signal applied at the output coupling region is bipolar. In our scheme illustrated in Fig. 3(a), $k_{b_1} \neq 0$ means a unipolar CLK signal and $k_{b_2} = 0$ implies a bipolar NRZ signal with constant amplitude. Following Eq. (7), the unipolar CLK signal will mix with the bipolar NRZ signal in the optical domain, which yields an optical signal with the waveform the same as that of the CLK signal and the phase alternating as the NRZ signal. In other words, the obtained optical signal is an optical RZ-PSK signal, as illustrated in Fig. 3(b). Second, $k_{b_1} = 0$ and $k_{b_2} \neq 0$, which suggests the CLK signal is bipolar and the NRZ signal is unipolar. Similarly, the mixing of the bipolar CLK and the unipolar NRZ in the optical domain will produce an optical CSRZ signal in Fig. 3(c). Third, if $k_{b_1} \neq 0$ and $k_{b_2} \neq 0$, both NRZ and CLK signals are unipolar, and pure RZ intensity

#160060 - $15.00 USD Received 15 Dec 2011; revised 31 Jan 2012; accepted 16 Feb 2012; published 20 Mar 2012

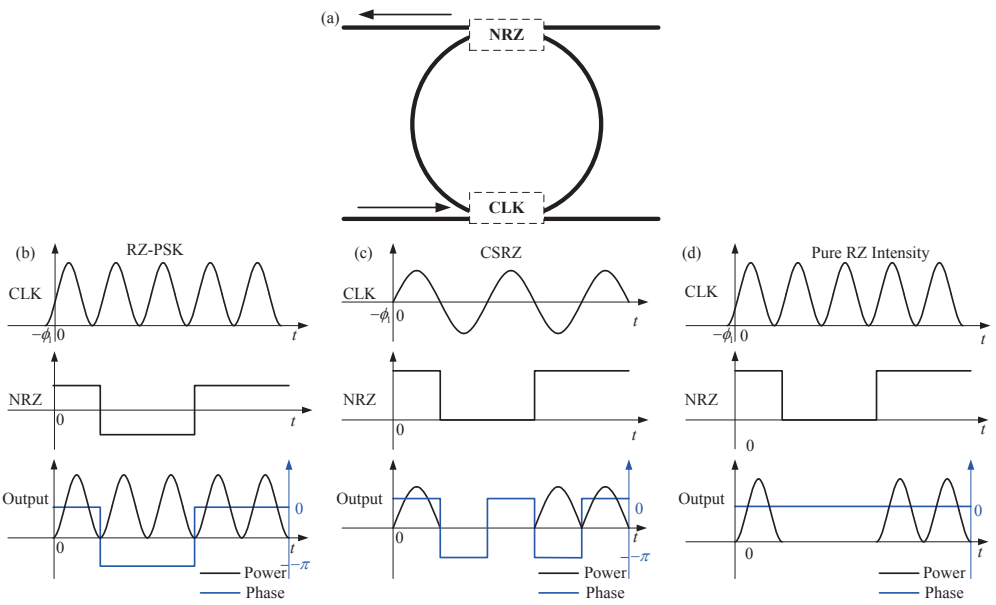

Fig. 3. (a) Signal application schemes for the proposed modulator. (b)-(d) Illustration of the advanced phase-shift of the CLK signal for (b) RZ-PSK, (c) CSRZ, and (d) pure RZ intensity modulations.

modulation in Fig. 3(d) can be implemented when $(1/\tau_l) \gg (v_g/2L)(k_{b_1}^2 + k_{b_2}^2)$ is satisfied. Again, $(1/\tau_l) \gg (v_g/2L)(k_{b_1}^2 + k_{b_2}^2)$ implies that the unloaded Q-factor of the modulator should satisfy the condition that $Q_0 \ll 1/[(2/\omega_0)(v_g/2L)(k_{b_1}^2 + k_{b_2}^2)]$, which can be deduced from the relation $1/Q_0 = 2/(\omega_0\tau_l)$ [10]. For example, if $k_{b_1} = 0.162$, $k_{b_2} = 0$, $\lambda_0 = 1551nm$, $L = 420\mu m$, the modulator should have an unloaded Q-factor of $Q_0 \ll 4 \times 10^5$. As indicated in Fig. 3(b)-(d), the signal applied to the input coupling region needs to be shifted with a phase-shift ϕ_1 in advance.

In summary, multiple optical chirp-free RZ modulation formats can be implemented by applying a CLK signal to the input coupling region and an NRZ signal to the output coupling region. Note that a phase-shift in advance is necessary for the signal applied to the input coupling region.

3. Simulation

Our proposed modulation scheme is essentially independent on the material platform that it can be built on. In particular, silicon-on-insulator (SOI) can be used due to its potential monolithic integration of photonic and electronic devices [11]. On the other hand, polymer materials, which have a much larger electro-optic coefficient and thus a lower driving voltage, can also be employed [12]. In our simulation, we assume the ring perimeter is 420 μm, and the length of the MZI arm is 200 μm. The ring waveguide propagation loss is $\alpha = 21\ dB/cm$, and the waveguide effective refractive index is $n_e \approx 2.5$. Here we assume the refractive index change is linearly proportional to driving voltage after the diode is turned on ($V_{th} = 0.7V$) and the effective index will have a change of 0.006 per volt according to the free carrier dispersion effect mentioned in [13]. We assume that the power of the input CW light is 0 dBm. The electrical NRZ signal is generated using a $2^7 - 1$ pseudo-random binary sequence (PRBS), and filtered

#160060 - $15.00 USD Received 15 Dec 2011; revised 31 Jan 2012; accepted 16 Feb 2012; published 20 Mar 2012

by a low-pass Butterworth filter to obtain a rising/falling time of 15 ps. To mimic the light wave propagation, we perform the simulation using the finite-difference method [14].

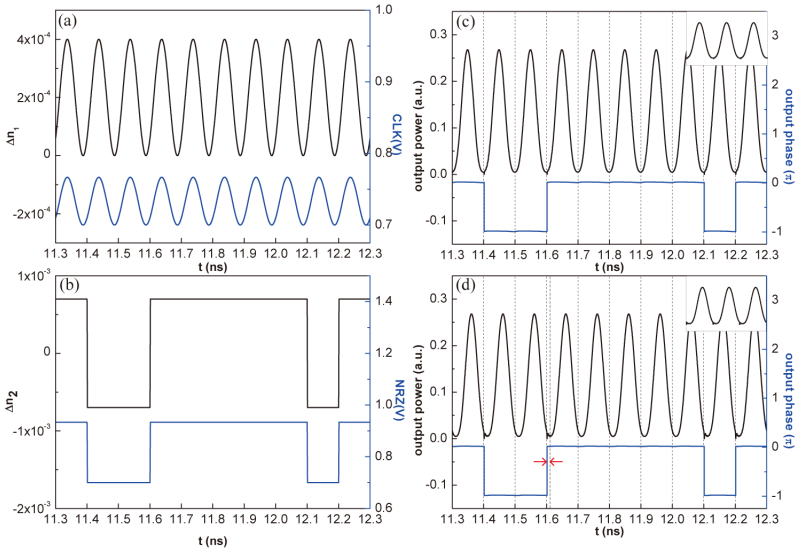

Fig. 4. (a) 10 GHz CLK driving signal and (b) 10 Gb/s NRZ driving signal for the RZ-PSK modulation. (c) Optical output signal when the CLK signal is phase-shifted in advance. (d) Optical output signal when there is no phase shift for the CLK signal. Insets in (c) and (d) show the output optical signal eye diagrams.

Figure 4 shows the performance for 10-Gb/s RZ-PSK modulation. The refractive index modulation Δn_1 and Δn_2 on the MZI couplers are shown in Fig. 4(a) and 4(b). The Δn_1 and Δn_2 modulation amplitudes (defined as the peak-to-peak value) are 4×10^{-4} and 1.4×10^{-3}, respectively. In this case, the microring operates at the over-coupling region. The phase-shift for the CLK signal is 0.25π. The driving voltages for the refractive index modulations are also indicated in the Fig. 4(a) and 4(b). Figure 4(c) shows the modulated optical signal with a power contrast ratio (CR) of larger than 17 dB and the phase of the output signal, which confirms the modulation is almost chirp-free. Our dynamic analysis in Section 2 shows that the CLK signal applied to the input coupling region suffers from a low-pass filtering effect. To suppress such an effect, we increase the amplitude of the NRZ signal to increase the output cross-coupling coefficient, and thus the Q-factor of the resonator is decreased. As visualized in Fig. 5, the CR of the output signal has a significant improvement from 7 dB to 23 dB when Δn_2 increases from 2×10^{-4} to 1.8×10^{-3}. Moreover, Fig. 4(d) shows the modulation performance in the scenario where the CLK signal isn't phase-shifted in advance. Figure 4(d) shows that there is misalignment between the output power waveform and the output phase waveform, which will increase the bit error rate at the receiver. This is consistent with the prediction by our analytical results in Subsection 2.2.

Figure 6 shows the result for the CSRZ modulation at 10-Gb/s, where the amplitude of Δn_1 is 8×10^{-4} and that of Δn_2 is 4×10^{-4}. The phase-shift for the CLK signal is 0.2π. In this case, the microring operates at the under-coupling region. Figure 6 illustrates that the resulting optical CSRZ signal has a large extinction ratio. We also find the optical CSRZ signal is nearly chirp-free except for a thorn-like phase peak at each 0-π transition. Such thorn-like phase peaks appear due to the fact that the propagation loss on each arm of the push-pull MZI couplers is slightly different. Fortunately, the thorn-like phase peaks correspond to a very low optical

#160060 - $15.00 USD Received 15 Dec 2011; revised 31 Jan 2012; accepted 16 Feb 2012; published 20 Mar 2012

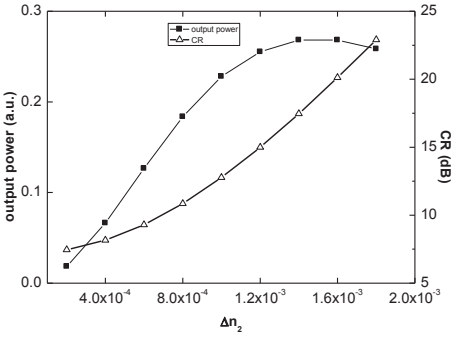

Fig. 5. Output power and CR change as a function of Δn_2 when the NRZ signal amplitude is varied.

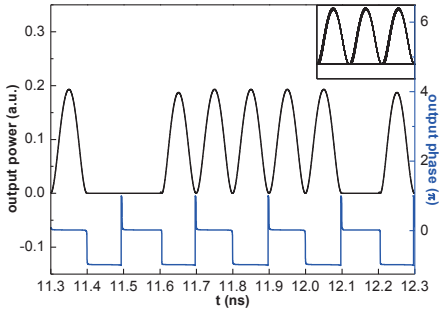

Fig. 6. Output optical signal power and phase for the CSRZ modulation at 10-Gb/s. Inset shows the optical signal eye diagram.

signal, and thus have a negligible effect.

Pure RZ intensity modulation can also be generated by applying a unipolar CLK signal and a unipolar NRZ signal to the input and output couplers, respectively. Figure 7(a) shows the modulated optical signals when the amplitudes of Δn_1 and Δn_2 are both 4×10^{-4}, and the CLK signal has a phase-shift of 0.35π. In this case, the microring operates at the under-coupling region. The resulting optical signal suffers from a little distortion. To reduce the distortion, we increase to 45 dB/cm to degrade the unloaded Q-factor of the modulator, while keeping the driving NRZ and CLK signals unchanged. Note that a more practical way to decrease the unloaded Q-factor is to introduce another waveguide to couple with the microring. Figure 7(b) shows the improved signal quality, which is consistent with our analysis. Note that the improvement in signal quality is at the expense of lower output signal power.

In practice, it is hard for the input wavelength to exactly match the resonance wavelength. Therefore, we investigate the impact of the wavelength deviation on the modulation performance of the proposed RZ modulator. The deteriorated modulation performances when a 0.01 nm wavelength deviation is introduced are shown in Fig. 8. It suggests that the modulated signals only incur a small chirp if the deviation is not very large.

4. Conclusion

We proposed an optical chirp-free RZ modulator based on a double coupled microring resonator. The static analysis suggests the output optical signal is resulted from the multiplication

#160060 - $15.00 USD Received 15 Dec 2011; revised 31 Jan 2012; accepted 16 Feb 2012; published 20 Mar 2012

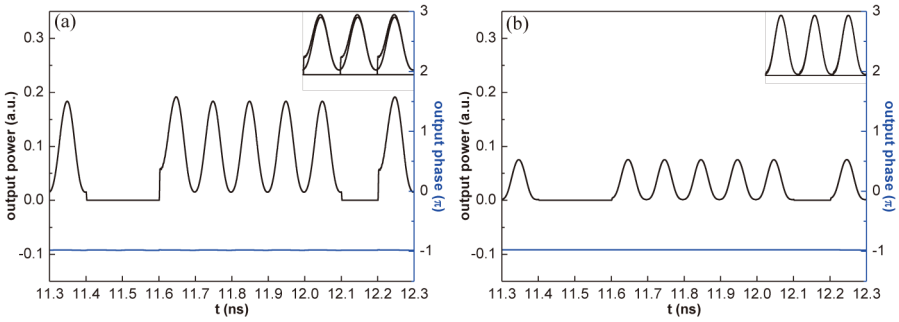

Fig. 7. Output optical signal power and phase for the RZ-intensity modulation at 10-Gb/s with the ring waveguide losses of (a) $\alpha = 21\ dB/cm$ and (b) $\alpha = 45\ dB/cm$. Insets show the optical signal eye diagrams.

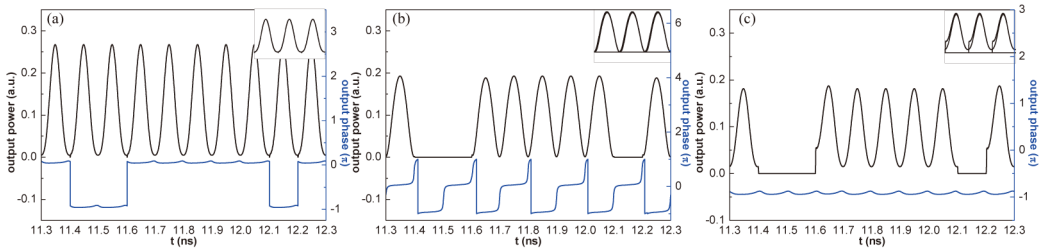

Fig. 8. Output modulated signals when input wavelength deviates from resonance by 0.01 nm for (a) RZ-PSK, (b) CSRZ, and (c) RZ-intensity modulations. Insets show the corresponding eye-diagrams of the modulated signals.

of two electrical signals (CLK and NRZ signals) applied to the input and output coupling regions. The time-domain CMT based dynamic analysis further reveals the modulation mechanism and the criteria for achieving RZ modulation are deduced. Due to the modulation bandwidth limitation at the input coupler, the CLK signal can only be applied to the input coupler and the NRZ signal to the output coupler. Multiple RZ modulation formats, such as RZ-PSK, CSRZ, and RZ intensity modulation, can be achieved by using different polarities of the applied electrical signals. We also did numerical simulations to confirm the feasibility of our modulator in realizing the various RZ modulation formats. The simulation results at 10 Gbit/s verify the feasibility of our proposed modulator for RZ-PSK, CSRZ, and RZ intensity modulations.

Acknowledgments

This work was supported in part by 973 program (ID2011CB301700), NSFC (61001074, 61071011, 61007039, 61127016), Project of MoE Key Lab of Optical Fiber Sensing & Communication (UESTC), The state Key Laboratory of Optoelectronics Project (No. 2010KFB002), STCSM Project (10DJ1400402), State Key Lab Projects (GKZD030004/09/15/20/21).

#160060 - $15.00 USD Received 15 Dec 2011; revised 31 Jan 2012; accepted 16 Feb 2012; published 20 Mar 2012